J Mater Sci: Mater Electron (2012) 23:753–757
DOI 10.1007/s10854-011-0484-9

Synthesis and characterization of sol–gel derived $(Ba,Ca)(Ti,Zr)O_3$ nanoparticles

Min Wang · Ruzhong Zuo · Shishun Qi · Longdong Liu

Received: 24 June 2011 / Accepted: 29 July 2011 / Published online: 7 August 2011

Abstract A citrate precursor method was employed to synthesize lead-free perovskite $0.5Ba(Zr_{0.2}Ti_{0.8})O_3$-$0.5(Ba_{0.7}Ca_{0.3})TiO_3$ (BZT-0.5BCT) crystallites. Powders and gels were characterized by X-ray diffraction, Fourier transform infrared spectroscopy, Raman spectra, thermal analysis and transmission electron microscopy. It was indicated that BZT-0.5BCT transparent gel can be obtained via the chelation of citric acid with metal ions. Gels transformed into crystalline powders with single-phase perovskite structure when heat-treated above 650 °C, significantly lower than that in a solid-state reaction method. The primary particle size of the powders increased from 30 to 60 nm as the decomposition temperature was raised from 600 to 750 °C.

1 Introduction

$BaTiO_3$ (BT) piezoelectric material has attracted extensive attention since its piezoelectric effect was disclosed half century ago. In recent years modified BT ceramics have been expected as alternative lead-free materials to traditional Pb-based piezoelectric ceramics. Particularly a huge piezoelectric effect was generated in Ca^{2+} and Zr^{4+} doped BT compositions such as $(1-x)Ba(Zr_{0.2}Ti_{0.8})O_3$-$x(Ba_{0.7}Ca_{0.3})TiO_3$ (BZT-xBCT) which was reported to have a piezoelectric coefficient of $d_{33} = 620$ pC/N at $x = 0.5$ [1]. Such excellent piezoelectric properties may open a way to the application of lead-free piezoelectric ceramics in some devices.

As far as the synthesis processing is concerned, the traditional solid-state reaction method was usually used to prepare BZT-xBCT perovskite powder and ceramics, which requires relatively high calcination temperature (1,350 °C) and sintering temperature (1,450–1,500 °C) [1]. However, this method is difficult to realize homogeneous distribution of compositions, sometimes leading to the appearance of impurity phases in addition to lower sintering activity of the synthesized powder. By comparison, soft-chemical routes, such as conventional sol–gel method, hydrothermal method, mechanochemical synthesis and sol–gel auto-combustion method, can effectively avoid these disadvantages owing to the control of accurate stoichiometry and the mixing of various liquid precursors on a molecular level [2–9]. Moreover, powders achieved by soft-chemical routes own significantly smaller particle size, leading to the improved densification behavior and electrical properties.

The citrate precursor method is an improved sol–gel processing in which not only would metal ions be chelated before the hydrolysis so that alkoxides or the formation of precipitates with metal ions be avoided, but also very fine multi-component oxide ceramic powders can be produced in a simple and economic way. In this study, a citrate sol–gel process was explored to prepare typical lead-free BZT-0.5BCT superfine powders. According to the literature survey, this attempt was not yet made so far although it has been used to prepare other lead-free piezoelectric compositions such as $(Bi_{0.5}Na_{0.5})TiO_3$ or $(Na_{0.5}K_{0.5})NbO_3$ based compositions [4, 5, 7, 8]. A special attention was focused on the chemical reaction and structural transformation behavior during the heat-treatment of the as-prepared xerogel by means of various characterization techniques.

M. Wang · R. Zuo (✉) · S. Qi · L. Liu
Institute of Electro Ceramics and Devices, School of Materials Science and Engineering, Hefei University of Technology, Hefei 230009, People's Republic of China
e-mail: piezolab@hfut.edu.cn

2 Experimental

The starting materials used in this study were $Zr(NO_3)_4 \cdot 5H_2O$ (≥99.0%), $Ca(NO_3)_2 \cdot 4H_2O$ (≥99.0%), $Ba(NO_3)_2$ (≥99.5%), $Ti(OC_4H_9)_4$ (≥98.0%), citric acid (≥99.5%) and ammonia (25–28%). All these chemicals are produced by Sinopharm Chemical Reagent Co., Ltd, China. Firstly, $Ti(OC_4H_9)_4$ diluted by ethanol was added into citric acid aqueous solution with pH ~8 which is adjusted by dripping appropriate amount of ammonia. After being stirred at 80 °C for 1 h, a yellowish transparent liquid was obtained which is marked as solution A. At the same time, inorganic compounds were dissolved into distilled water, accompanying uninterrupted stirring until all salts were absolutely solved which is marked as solution B. Subsequently, solutions A and B were poured together. At the same time the pH value was adjusted to be ~7 using ammonia till a transparent liquid was achieved. The molar ratio of citric acid to metal cations was 1.25:1. Followed by a continuous stirring for 3 h, the viscosity of solution increased gradually and then a stable transparent sol formed. The sol was heated at 120 °C to remove redundant solvent and was finally converted into gel. The gel was pretreated at 220 °C and then underwent heat treatment at various temperatures for 4 h. The flow chart of the procedure mentioned above is displayed in Fig. 1.

Thermo-gravitometry (TG) and differential scanning calorimetry (DSC) analysis of the as-prepared gel was carried out by using a simultaneous thermal analyzer (STA409C, Netzsch, Germany). The structural evolution of xerogel and powders heat-treated at different temperatures were analyzed by Fourier-transform infra-red spectrum (FT-IR, Spectrum 400, PerkinElmer, USA). The powders heat-treated at different temperatures were characterized by an X-ray diffractometer (XRD, D/MAX2500 VL/PC, Rigaku, Japan) with Cu Kα radiation and a Raman spectrometer (LabRAM HR800, HJY, France) for the crystallization state and crystal lattice vibration. The morphology, grain size and Selected Area Electron Diffraction (SAED) of the as-synthesized particles were analyzed by means of a high-resolution transmission electron microscope (HR-TEM, JEOL-2010, JEOL, Japan).

3 Results and discussion

Figure 2 shows the TG and DSC curves of the BZT-0.5BCT gel. The small endothermic peak at ~201 °C and the exothermic peak at ~296 °C are due to the evaporation of water, ethanol, ammonia, some organic impurities and the combustion heat of superfluous citrate acid, respectively, accompanied by a mass loss of ~37.1% in TG curve. The following 9.7% mass loss between 300 and 450 °C was attributed to the thermal decomposition of citrate chelate compounds resulting from the complexation reaction. The strongest exothermic peak at ~476 °C could be related to the combustion of nitrate and residual organic components. The gentle exothermic peak at ~586 °C may be correlated to the initial crystallization temperature according to the previous work about BT [10]. After ~25% mass loss during 450–700 °C, most of organic compounds have been eliminated so that no obvious weight loss or peaks can be seen thereafter in the TG and DSC curves, indicating that the thermal decomposition and structur adjustment of the BZT-0.5BCT gel are almost completed before 700 °C.

The structural evolution of the gel with the increase in heat-treatment temperature was characterized by FT-IR as shown in Fig. 3. The absorption spectra of the gel should be helpful to detect the interaction among organic groups. The broad bands at 3,440 and 3,170 cm^{-1} correspond to the stretching of O–H in water molecule or citric acid [11], which tends to disappear above 500 °C. However, the O–H stretching band at 3,440 cm^{-1} still appears in the sample

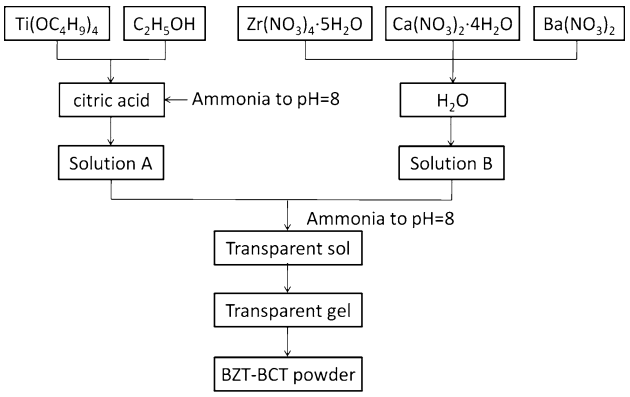

Fig. 1 The flow chart of the citrate sol–gel processing for BZT-0.5BCT powders

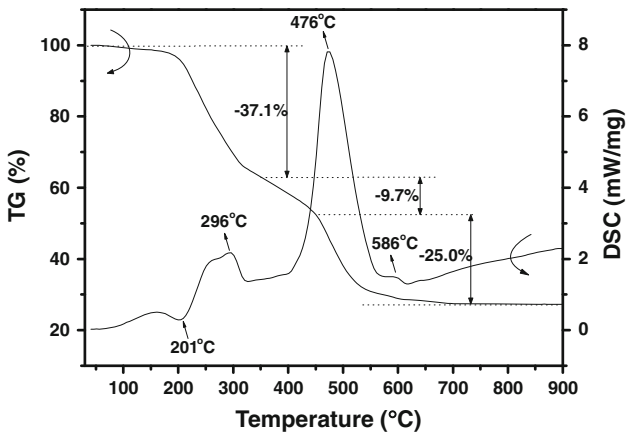

Fig. 2 TG-DSC curves of BZT-0.5BCT gel

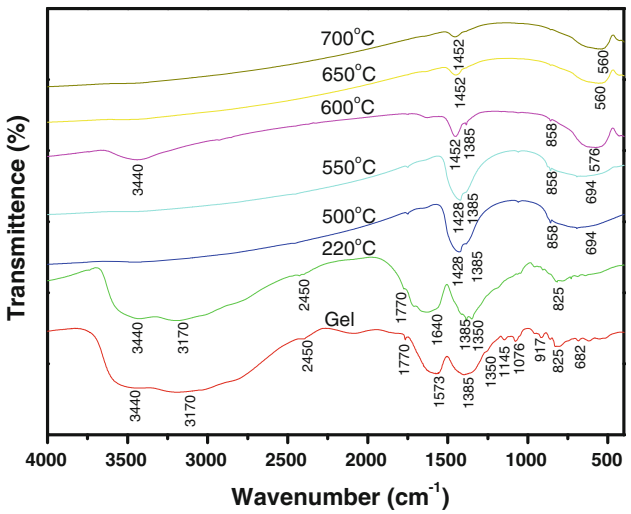

Fig. 3 FT-IR spectra of BZT-0.5BCT gel and powders heat-treated at different temperatures

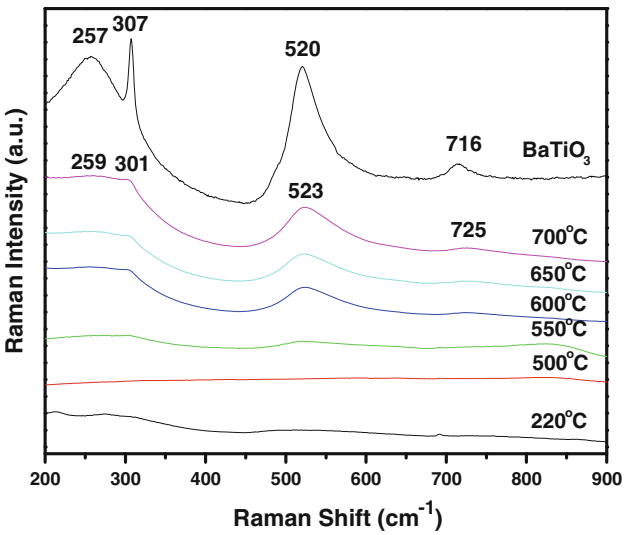

Fig. 4 Room-temperature Raman spectra of the BCT-0.5BZT gel powders heat-treated at different temperatures and $BaTiO_3$ powder calcined at 700 °C

calcined at 600 °C, which may be attributed to little moisture absorbed by unstable intermediate phase on cooling [12]. The peaks at 2,450 and 1,385 cm^{-1} are both caused by the C–H stretching vibration. The peak at 1,770 cm^{-1} is related to the C = O stretching in carbohydrates and the peaks at 1,350, 1,145 and 1,076 cm^{-1} are assigned to the C–O stretching, meaning that carboxylic groups exist at various states. This further indicates that the esterification has completed and metal ions have changed into stable bidentate-ligand complexes [13]. The peaks at 1,428 and 917 cm^{-1} are dependent on the in-plane bending and out-of-plane bending of C–O–H, respectively. They totally disappear above 500 °C, which keeps consistent with TG-DSC results. The bands at 1,573, 825 and 694 cm^{-1} could be identified as the stretching and bending of N–O bonds from NO_3^-. After heat treatment, the bands related to citrate and nitrate get reduced or disappeared or even shifted probably because of less restriction by other groups, for example, N–O bands at 825 shift to 858 cm^{-1}. It is interesting to note that two new peaks at 1,428 and 1,385 cm^{-1} combine into one at 1,452 cm^{-1}, which could be considered as M–O–C (metal ion- oxygen-carbon) [14]. The appearance of a broad band at 560 cm^{-1} due to the stretching vibration of Zr–O and Ti–O confirms the formation of a perovskite structure, which can be also proved by the following XRD results.

Raman spectra of as-prepared powders are shown in Fig. 4 in order to deeply explore the phase structural transformation of the gel powders undergoing the heat treatment as the Raman result can help detect molecular vibrations directly and is very sensitive to non-uniform distortions of the crystal lattice in short-range ordering [15]. It can be found that no Raman activity is visible below 500 °C, since atoms were only randomly arranged at this moment and the perovskite structure has not yet been created. As the calcination temperature rises to 550 °C, the characteristic Raman peaks of a perovskite structure begin to appear. As the calcination temperature is 600 °C or more, the Raman peak is more evident, hinting that perovskite unit cells have formed. Similar to BT, the effective vibration modes of BZT-0.5BCT powder is $3(A_1+E)+E+B_1$ [16]. But at the presence of long-range electrostatic forces, each of the A_1 and E modes further splits into transverse (TO) and longitudinal (LO) optical modes. Chang et al. [17] consider that the phonon vibration of the Ba–O bonds in BT are closely related to the formation of 517 and 718 cm^{-1} bands, and that Ti–O bonds to the formation of 257 and 307 cm^{-1} bands and similar

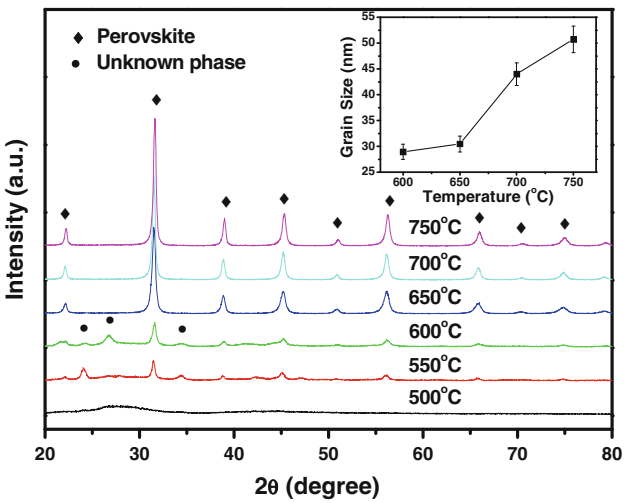

Fig. 5 XRD patterns of BZT-0.5BCT gel powders heat-treated at different temperatures

result was obtained from BT powder, which was prepared by citrate sol–gel processing and heat-treated at 700 °C. As for BZT-0.5BCT, the feature is that a broad peak centered near 259 cm^{-1} and a faint peak at 301 cm^{-1} originate from A_1(TO) mode and [B_1, E(TO+LO)] mode, respectively, which move to lower frequencies as compared to BT. An asymmetric and dominant peak near 523 cm^{-1} is [A_1, E(TO)] mode and a broad and small peak at around 725 cm^{-1} is [A_1, E(LO)] mode, both of which shift to higher frequency compared to pure BT. The origin of band shift lies in different ion radius between Ba^{2+} and Ca^{2+} as well as Ti^{4+} and Zr^{4+} which tends to lead to the distortion and disorder of the lattice and further results in energy band widening [18]. These results further prove that Zr^{4+} and Ca^{2+} ions have entered into the BT lattice.

The XRD patterns of BZT-0.5BCT powders heat-treated between 500 and 750 °C are shown in Fig. 5. It can be seen that there is only a broad and faint peak below 500 °C, although powders look white under such temperature. That is to say, carbonaceous organic materials have been combusted but powders still exhibit typical patterns of amorphous phases, which is consistent with the Raman spectrum. As the temperature reaches 550 °C, the typical diffraction peaks for a perovskite structure start to appear

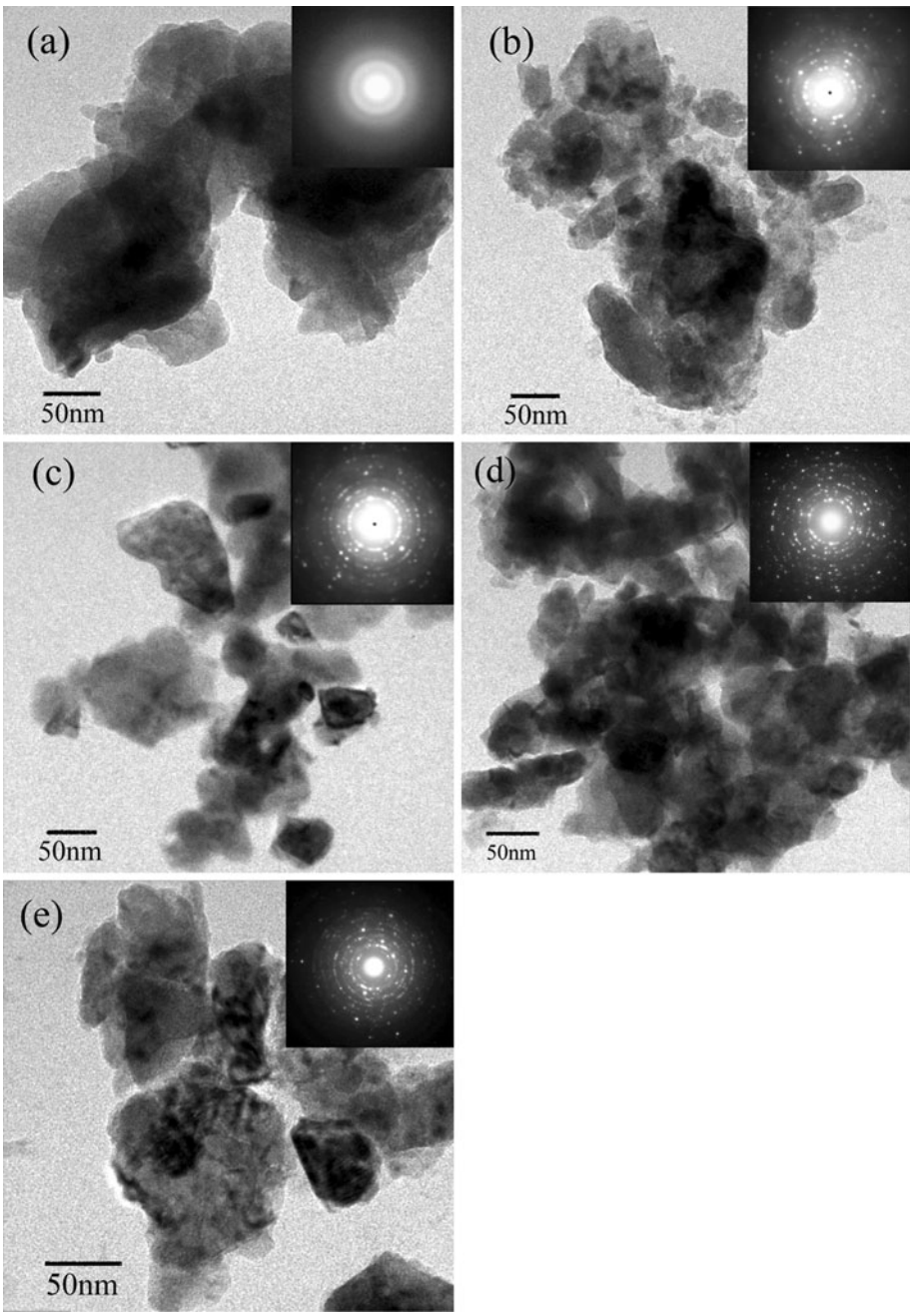

Fig. 6 TEM photograph of BZT-0.5BCT heat-treated at various temperatures: **a** 500 °C, **b** 550 °C, **c** 600 °C, **d** 650 °C, and **e** 700 °C. The insets are the corresponding SAED patterns

but coexisted with peaks of unknown intermediate phases. Pure cubic perovskite structure forms till 650 °C at which nitrate and citrate are absolutely removed based on the analysis of FT-IR and TG-DSC. It can be affirmed that BZT-0.5BCT crystalline powder can be well synthesized below 700 °C by the citrate sol–gel method, which is much lower than that by a solid-state reaction method (1,350 °C) [1]. Furthermore, the particle size of as-prepared powders can be estimated according to Scherrer formula [7]: $d = \frac{k\lambda}{B\cos\theta}$, where d is the grain size; k the Scherrer constant; λ the X-ray wavelength ($\lambda = 0.154056$); θ the diffraction angle; B the Full Width of Half Maximum of the diffraction peak. The calculated grain size is in the range of 30–60 nm as inset in Fig. 5. It increases gradually with the calcination temperature.

Figure 6 shows the particle morphology of sol–gel derived BZT-0.5BCT powders heat-treated at various temperatures. In Fig. 6a and b, large pieces of agglomerated particles can be seen, owing to the adhesion of organic matters as confirmed by TG-DSC and FT-IR results. Polygon-like particles are visible when the heat-treatment temperature is 600 °C. At 650 °C, particles show an average diameter of ~50 nm, which seems slightly larger than the calculated value probably because of the agglomeration of the powder. Particles obtained at 700 °C exhibit serious adhesive phenomenon owing to relatively higher calcination temperature. The inset picture is the corresponding SAED obtained from the diffraction of several grains. Circular diffraction pattern representing non-crystalline structure is visible at 500 °C due to the absence of crystalline phases. However, the polycrystalline diffraction circles composed of discrete spots tend to be distinct as heat-treatment temperature increases, illuminating that the perovskite structure forms gradually.

4 Conclusions

Lead-free perovskite BZT-0.5BCT nano-scaled powders have been successfully synthesized by a citrate sol–gel method. The chemical reaction and structural transformation behavior during heat-treatment of as-prepared xerogels were characterized by FT-IR and Raman spectra, TG-DSC, XRD and TEM. The results showed that the crystallization temperature of the gel was reduced by ~700 °C as compared to that in a mixed-oxide route. Crystallites with pure perovskite structure and a particle size of 30–60 nm can be obtained by using appropriate calcination temperatures.

Acknowledgments This work was financially supported by the Fundamental Research Funds for the Central Universities, and by the National Natural Science Foundation of China (50972035) and a Program for New Century Excellent Talents in University, State Education Ministry (NCET-08-0766).

References

1. W.F. Liu, X.B. Ren, Phys. Rev. Lett. **103**, 257602 (2009)
2. H.A.M. van Hal, W.A. Groen, S. Maassen, W.C. Keur, J. Eur. Ceram. Soc. **21**, 1689 (2001)
3. X.Z. Jing, Y.X. Li, D.R. Yin, Mater. Sci. Eng. B **99**, 506 (2003)
4. Q. Xu, X.L. Chen, W. Chen, S.T. Chen, B. Kim, J. Lee, Mater. Lett. **59**, 2437 (2005)
5. J.G. Hou, Y.F. Qu, W.B. Ma, D. Shan, J. Mater. Sci. **42**, 6787 (2007)
6. E. Mercadelli, C. Galassi, A.L. Costa, S. Albonetti, A. Sanson, J. Sol. Gel. Sci. Technol. **46**, 39 (2008)
7. C. Wang, Y.D. Hou, H.Y. Ge, M.K. Zhu, H. Yan, J. Eur. Ceram. Soc. **29**, 2589 (2009)
8. H.Q. Wang, R.Z. Zuo, Y. Liu, J. Fu, J. Mater. Sci. **45**, 3677 (2010)
9. W. Li, Z.J. Xu, R.Q. Chu, P. Fu, J.G. Hao, J. Alloys Compd. **482**, 137 (2009)
10. Q.A. Harizanov, Mater. Lett. **34**, 232 (1998)
11. B. Stuart, *Infrared Spectroscopy: Fundamentals and Applications* (Wiley, UK, 2004)
12. E.M.A. Hamzawy, A.F. Ali, Ceram. Int. **27**, 607 (2001)
13. H. Kozuka, *Handbook of Sol-Gel Science and Technology: Processing, Characterization and Applications, vol. I Sol-Gel Processing* (Kluwer, Netherlands, 2005)
14. R.M. Almeida, *Handbook of Sol-Gel Science and Technology: Processing, Characterization and Applications, vol. II Characterization and Properties of Sol-Gel Materials and Products* (Kluwer, Netherlands, 2005)
15. Y.P. Guo, K. Kakimoto, H. Ohsato, Appl. Phys. Lett. **85**, 4121 (2004)
16. U.D. Venkateswaran, V.M. Naik, R. Naik, Phys. Rev. B **58**, 14256 (1998)
17. M.C. Chang, S.C. Yu, J. Mater. Sci. Lett. **19**, 1323 (2000)
18. Q.Y. He, X.G. Tang, J.X. Zhang, M.M. Wu, Nanostruct. Mater. **11**, 287 (1999)